

# CONCLUSIONS FROM ESA SPACE DEBRIS TELESCOPE OBSERVATIONS ON SPACE DEBRIS ENVIRONMENT MODELLING

H. Krag<sup>1</sup>, H. Klinkrad<sup>1</sup>, R. Jehn<sup>1</sup>, S. Flegel<sup>2</sup>, T. Schildknecht<sup>3</sup>

<sup>1</sup>ESA/ESOC Space Debris Office, Robert-Bosch-Str. 5, D-64293 Darmstadt, Germany, Email: [holger.krag@esa.int](mailto:holger.krag@esa.int), [heiner.klinkrad@esa.int](mailto:heiner.klinkrad@esa.int), [ruediger.jehn@esa.int](mailto:ruediger.jehn@esa.int)

<sup>2</sup>Institute of Aerospace Systems, TU Braunschweig, Hermann-Blenk-Str. 23 D-38108 Braunschweig, Germany, Email: [s.flegel@tu-bs.de](mailto:s.flegel@tu-bs.de)

<sup>3</sup>AIUB, Sidlerstr. 5, CH-3012 Bern, Switzerland, Email: [thomas.schildknecht@aiub.unibe.ch](mailto:thomas.schildknecht@aiub.unibe.ch)

## 1. ABSTRACT

Population-based space debris environment models, like ESA's MASTER (Meteoroid and Space Debris Terrestrial Environment Reference), make use of release models for the different source terms in order to generate a space debris population to a certain size threshold. Detailed information on break-up events, like the fragmented mass and its orbit at event epoch, are required for that purpose. Such information is typically generated by the the US Space Surveillance Network, which identified all major fragmentation events in LEO. However, the sensitivity threshold of the US Space Surveillance in GEO is significantly lower (at about 1m object size compared to 10cm in LEO), so that today, only two fragmentation events in GEO have been confirmed. In 2001, the ESA Space Debris Telescope (ESA SDT) became operational. It is a 1m Ritchey-Chrétien telescope at the ESA Optical Ground Station on Tenerife. During 7 years of operation, the ESA SDT has carefully screened the GEO environment and detected a large population of objects of sub-meter size, that cannot be explained from the two known fragmentation events alone. Furthermore, a number of objects have non-typical high area-to-mass ratios. Also, a number of objects were detected on eccentric, GTO-like orbits, sometimes even highly inclined. This paper analyses potential sources for those detections, such as unknown fragmentation events on GEO and GTO, contributions from fragmentations on Molniya-type orbits, and the release of multi-layer insulation (MLI) pieces. Such debris release events will be simulated using the modelling principles of MASTER-2005 extended by a dedicated approach for MLI release. The modelling results will be compared with the ESA SDT data for various epochs in order to estimate event epoch and in order to calibrate the imparted velocities from the evolution of the clouds. For this comparison, a dedicated software, PROOF-2005 (Program for Radar and Optical Observation Forecasting) will be used. It simulates space debris observation campaigns for given sensors observing the MASTER model population. A particular point of interest are potential insights into the release mechanisms of MLI fragments, which could be

either due to delamination or fragmentation of the corresponding spacecraft or orbital stage. This might be traceable, to some degree, through the orbital distribution of these objects. Finally, we will present a process to identify the most likely number and character of fragmentation and release events in GEO and GTO and its results will be presented in detail.

## 2. INTRODUCTION

Since 1995, ESA maintains and publishes the "Meteoroid and Space Debris Terrestrial Environment Reference" (MASTER) model. It has been issued first in 1995 and is continuously improved with the current release being MASTER-2005 [2]. MASTER determines flux information with high spatial resolution from an object population derived from historic debris generation events. These comprise more than 190 on-orbit fragmentation events, more than 1,000 solid rocket motor firings, and 16 reactor core ejections of RORSAT satellites [2]. The model is used to assess the debris or meteoroid flux imparted on a spacecraft on an arbitrary Earth orbit.

This purely modelling based approach requires observation data for its validation and calibration. Optical instruments, the sensitivity of which is less range dependent than for radars, installed at low latitudes are best suited for such kind of observations. To initialise European activities in the field of optical debris observations, ESA installed a Zeiss telescope system in the Optical Ground Station (OGS) at the Observatory of the Teide in Tenerife, Canary Islands. This observatory is located on top of the mountain Izaña (2393 m) about 20 km northeast from Teide, the highest mountain of Spain. The site is known for its excellent seeing conditions. This telescope, also dubbed "ESA's Space Debris Telescope" (ESASDT) is a classical astronomical telescope with a 1-meter primary mirror and an English mount. For debris observations the modified Ritchey-Chrétien focus is equipped with a CCD camera. The focal plane array consists of a mosaic of four 2k x 2k pixel CCDs. The total field of view is

about  $0.7 \times 0.7$  square degrees and the pixel size corresponds to 0.6 arcseconds. The CCDs are cooled with liquid nitrogen to 160 K to reduce the dark signal produced by thermal motion. In order to achieve short read-out times, each CCD chip is equipped with two readout channels. Each CCD is controlled by a separate amplification and digitization unit. The shortest readout time for a full image is 19 s. The readout noise level for the camera is 4-6 electrons per pixel at the fastest readout speed. This allows detection of 20–21 magnitude objects with 1–2 second exposures.

The ESASDT is used in survey mode for the search and initial orbit determination of new object and in follow-up mode for the refinement of the orbit information in order to maintain a temporal catalogue of objects. The results of the observations in survey mode, despite of their statistical character, are of particular importance to the validation and calibration of the environment models. They may, however, not be used in a direct sense, since measurements are always the result of a filtering process according to the particular sensor characteristics and the observation geometry. Hence, an extrapolation from measurements to a complete population for comparison with the model is not feasible when the circumstances under which the measurements have been generated are ignored. Also many measured parameters like range-rate and RCS are not available in the model. ESA's approach therefore consists of the conversion of the model population into detected objects by letting it undergo the same filtering process like the real objects. This is implemented through the computer code PROOF (Program for Radar and Optical Observation Forecasting). PROOF is simulating the objects passage through a sensor's field of view, reflecting the properties of the sensors in accurate sensor performance models and generating the same physical parameters for each detection as the real sensors [1]. This provides a consistent base for the comparison of measurements and models. PROOF can also predict object passage and detection probabilities for catalogued objects which is meant to support instrument operators in the correlation of detected objects.

## 2. MODELLING THE GEO ENVIRONMENT

The modeled fragment population used by MASTER is based on simulation of fragmentation events considering distribution laws for size, delta-velocities, area-to-mass and mass. These distribution laws have been adopted from the NASA break-up model (with some modifications). The simulation considers particle sizes down to one micrometer. The resulting object clouds for the event epoch are then propagated to the epochs of interest. The NASA break-up model has been validated

against both, on-ground experimental fragmentations of representative objects and the radar observation of fragment orbits generated during real events. The model provides information on diameter distribution, object cross-section and mass. Like all break-up models it assumes an isotropic distribution of delta-velocities. The simulation process relies on a list of fragmentation events, each specified with fragmenting mass, target orbit and event epoch. This list is based on the information provided in [4], which by today contains only two confirmed fragmentation events for GEO (see Table 1).

Table 1: Known fragmentation events in GEO

Name	COSPAR-ID	Mass [kg]	Event epoch	a [km]	i [deg]
Titan Transtage	1968-081E	1487	21-Feb-92	41833	11.9
Ekran 2	1977-092A	1952	25-Jun-78	42171	0.1

Another Titan Transtage break-up (1967-066G) was suspected to have occurred in February 1994 (33,254km x 33,676km @ 11.67°) [3]. Besides fragmentations on GEO, also fragmentations on GTO and even Molniya orbits can lead to a short-term presence of fragments in GEO altitudes. The parent orbits of these objects are displayed in Figure 1. One can see that at least 31 fragmentations are known to have occurred on Molniya-type orbits and at least 27 fragmentations have occurred on GTO orbits. The latter includes GTO with higher inclinations (up to 52.01°) for objects which have been launched from Russian sites.

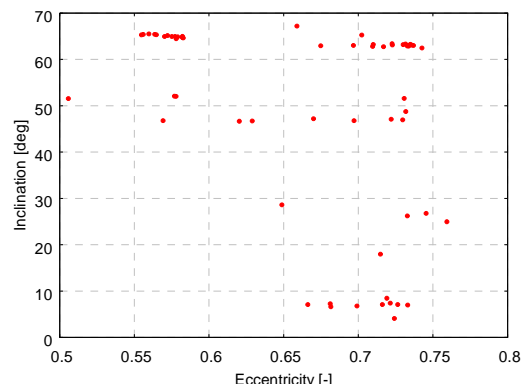


Figure 1: Orbits of fragmented objects with eccentricities  $> 0.5$  and  $< 0.8$

Figure 2 present a series of snapshots out of the history of the environment in high altitudes. The right ascension of ascending node (RAAN), inclination and eccentricity of objects  $> 10$ cm in orbits intersecting the GEO protected zone are shown. Uncontrolled objects on the geostationary ring will remain on near-circular orbits, however, inclination will build-up as a consequence of luni-solar perturbations acting on the orbit. This has also an effect on the RAAN angle which changes as a

function of the inclination. The resulting effect is an oscillation of the orbital plane normal around  $\alpha = 180^\circ$  and  $\delta = 77.5^\circ$ , with a period of 52 years and an amplitude of  $15^\circ$  in inclination. One can identify the clouds of the three known fragmentation events in GEO, as they follow this pattern of motion. The first fragments have gone through half of this cycle at around 1996 and their inclination is now decreasing again. The fragments on Molniya orbits can be found inside an inclination band around  $65^\circ$ . The angular change rate of the RAAN is much higher than for GEO objects and their inclination is fairly constant. The same holds for the GTO fragmentation (at around  $28^\circ$  and below  $10^\circ$  inclination) which set-in later.

In the following, the long-term evolution of fragment clouds on highly inclined and highly eccentric orbits will be analysed. Such orbits are only able to contribute to the GEO environment if the argument of perigee is either close to  $0^\circ$  or close to  $180^\circ$  and the apogee radius is exceeding the radius of the GEO ring. All orbits are subject to the rotation of the line of apsides which is caused by gravitational perturbations induced by the flattening of the Earth ( $J_2$ ). The only exceptions are orbits with inclination of  $63.4^\circ$ , for which the mentioned gravitational perturbations have no effect. This is exploited for the so-called Molniya orbits ( $1000\text{km} \times 39,357\text{km} @ 63.4^\circ$ ), which have revolution time of 0.5 sidereal days with the apogee stabilized over Russia, so that twice a day, the satellite is visible from that region for a period of several hours.

The evolution of such orbits has been studied in Figure 3. This analysis is based on the propagation of a fragment with  $A/m = 1\text{m}^2/\text{kg}$  over a period of 50 years.

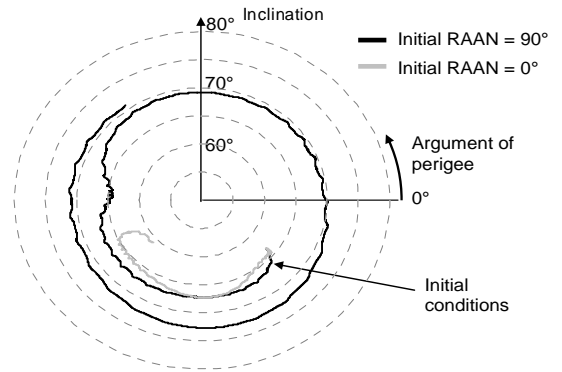


Figure 3: Evolution of Molniya orbits ( $A/m = 1\text{m}^2/\text{kg}$ ) over 50 years

Since the orbital evolution and lifetime depends on the attitude of the orbital plane, two initial conditions for the right ascension of the ascending node have been studied. The initial argument of perigee of Molniya is typically at around  $320^\circ$ . One can depict that fragments generated on Molniya-type orbits will experience an increase in inclination. The reasons for this are the 3rd-body perturbations due to Sun and Moon. As a consequence, the argument of perigee will become unstable and geopotential perturbations (Earth flattening) will cause the line of apsides to drift in negative direction. Accordingly, the apogee part of the

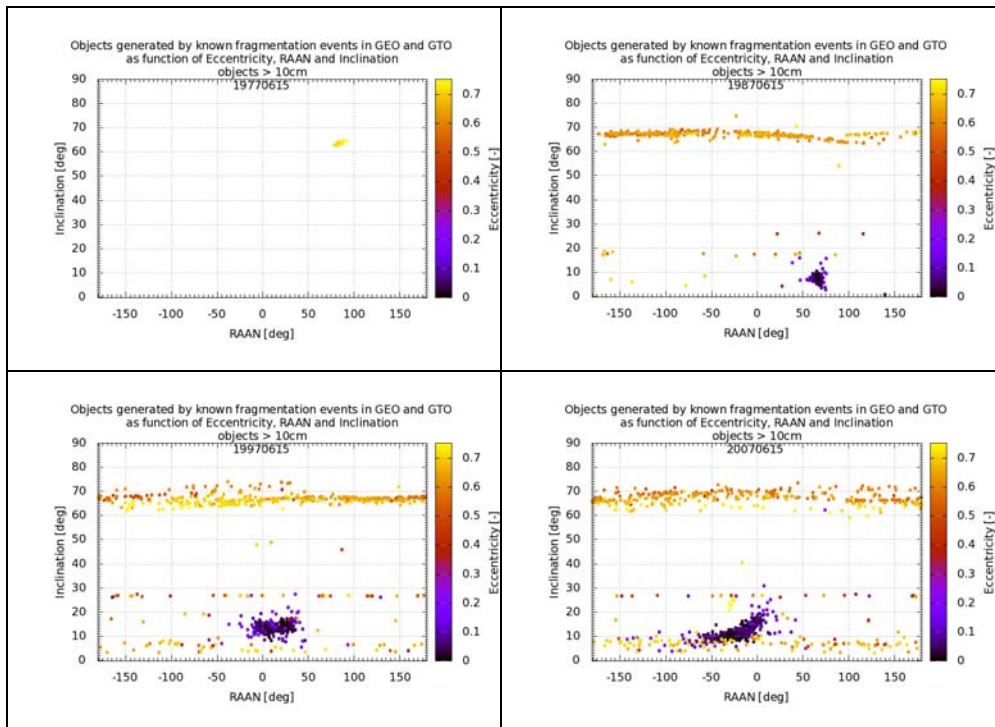


Figure 2: Snapshots of the orbital distribution of objects  $>10\text{cm}$  in GTO and GEO (as per MASTER-2005) in 1977, 1987, 1997 and 2007 (from upper left to lower right)

orbits will periodically intersect the GEO protected region. The GEO protected region is a definition of the Inter-Agency Debris Coordination Committee (IADC) which describes the volume around GEO bounded by  $\Delta h = \pm 200\text{km}$ ,  $\Delta\delta = \pm 15^\circ$ . As can be also depicted, this is only the case for particular initial orbital planes, as objects tend to decay for many other cases.

The fragmentation events on these orbits have been simulated according to the specifications and the chronology given in [2]. The results for two snapshot epochs are given in Figure 2 displaying the Argument of Perigee and the Right ascension of the ascending node. The dispersion of the RAAN due to the initial conditions and the nodal drift leads to the fact that Molniya fragments will be visible also from the longitude where the ESASDT is installed.

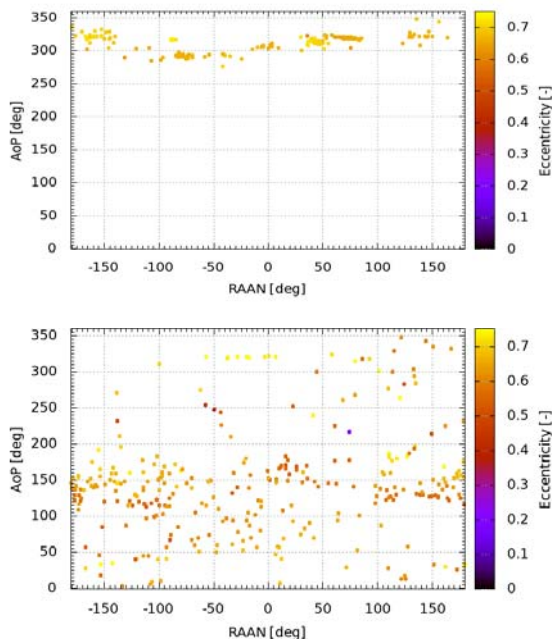


Figure 4: Distribution of Molniya fragment orbits in 1977 (top) and 2007 (bottom)

The contribution of these fragments to the spatial density in the GEO protected region has been compared to the contribution of fragments on GTO and GEO. Table 2 shows the results for objects  $> 1\text{cm}$ . It is remarkable, that, based on confirmed fragmentations, the contribution of Molniya objects is comparable to that of GTO objects. Obviously, the large number of fragmentations and the higher perigee of the Molniya events can compensate the short transition times through the GEO protected region. However, one must keep in mind that also higher inclined GTOs (Proton and Cape Canaveral launches) have substantial periods where the line of apsides does not allow any intersection with the GEO protected region. In total, however the contribution of fragments on eccentric orbits to the GEO environment is insignificantly small.

Table 2: Contribution of fragment groups to the spatial density in the GEO protected region

Class	Contribution
GEO objects	99.91%
GTO objects	0.04%
Molniya objects	0.05%

### 3. Comparison to Measurements

#### 3.1. ESA Space Debris Telescope Observations

Since 2004, the surveys conducted with the ESA space debris telescope concentrate on both, GEO and GTO orbits. Surveys screen an inertially fixed search field, in a right ascension/declination direction where the highest density of fragments can be expected. During exposures the telescope follows the expected motion of the objects (blind tracking). This measure concentrates the light received from the objects on a few pixels which improves the signal to noise ratio and simplifies the detection of objects, as the images of the stars are forming trails. The tracking velocity of geostationary corresponds to the sidereal motion ( $15''/\text{s}$ ). GTO objects are expected to be observed around their apogee passage where they appear significantly slower compared to GEO objects ( $7.5''/\text{s}$ ). As the apogee altitude of GTO orbits is decreasing with time, its apparent motion in the apogee region will increase. To encounter the problem of GTO orbit degradation, two GTO survey types are defined which leads to the overall definition of surveys.

- GEO surveys:  $15''/\text{s}$  blind tracking in right ascension
- GTO-75 surveys:  $7.5''/\text{s}$  blind tracking in right ascension (for exact GTOs with 2.26 rev/day)
- GTO-105 surveys:  $10.5''/\text{s}$  blind tracking in right ascension (for degraded GTOs with 3 rev/day)

Table 3 gives a summary of the observation hours dedicated to the three survey types.

Table 3: Observation hours of the ESA SDT spent per survey types

Survey type	2004	2005	2006	2007
GEO	177h	149h	130h	89h
GTO75	85h	110h	125h	75h
GTO105	62h	98h	111h	107h

Figure 5 shows the inclination and right ascension of ascending node of the uncorrelated detections of the year 2005. The coupled inclination/RAAN perturbation of uncorrelated geostationary objects with the maximum amplitude of  $15^\circ$  in inclination is visible in particular as a result of the GEO surveys. GTO surveys lead to the discovery of objects outside of this band but (in particular for the GEO105 surveys) discovered geostationary objects as well.

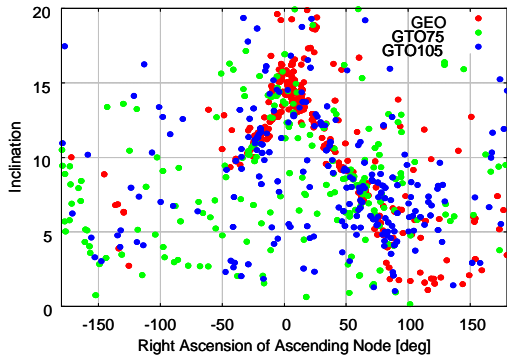


Figure 5: Orbital parameters of uncorrelated objects detected in 2005 as a function of the service type

### 3.2. Comparison for the known fragments

Figure 6 overlays the modeling results for the three known fragmentations as processed by PROOF for the survey fields of 2005 for uncorrelated detections. The ESA telescope detected 928 objects in this year which compares to only 115 detections predicted by PROOF.

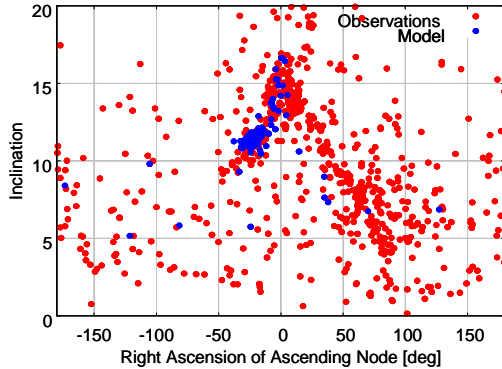


Figure 6: Observed and modeled uncorrelated objects for the search fields of 2005

Qualitatively the modeled fragment clouds of the three fragments seem to match well with the relevant detections by the telescope. This underlines the correctness of fragmentation model and PROOF, which translates the modeled fragment clouds into simulated telescope detections. However, it is obvious that a large number of uncorrelated detections cannot be explained. As most of the detection appear in clusters that show similar features as the correlated clouds, unknown fragmentation events are a likely explanation.

It is essential for a space debris model to be in good alignment with measurements. As MASTER is based on deterministic source models it requires well-defined events to compensate the gap. Therefore an attempt has been made to introduce a series of additional events that are defined such that they provide an optimum match with the measurements. These events do not have any justification nor do they correlate with any existing

object. Such attempts to improve the model by additional (artificial) events have been performed already before in [1] and later improved in [3], however, with the availability of measurement data another refinement is possible. A particular difficulty in defining these events consists in the ambiguity between epoch of the event and the epoch of loss-of-control of the progenitor object. For example, the mean orbital elements of a fragment cloud of an object that broke up 10 years ago on the geostationary ring would, be close to that of an object for which control was lost ten years ago but that broke up just today. Here, an analysis of the shape of the cloud can, to some degree, be helpful. This is not an unambiguous indicator, but the correct pattern can be adjusted by the selection of the epoch in combination with, as Figure 7 shows, the position of the event on the geostationary ring.

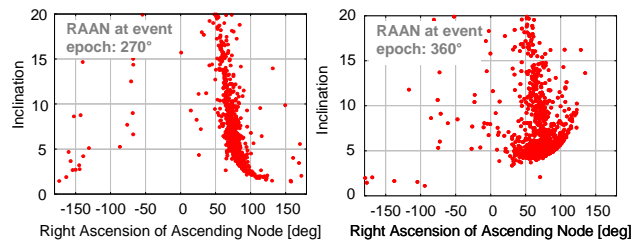


Figure 7: Fragment clouds from fragmentation events on GEO orbits (with different RAAN, i.e. on-orbit position) 6 years after the event

It was also found important to verify the results any progenitor orbit over several years (as far as measurements are available), since the evolution of the cloud shape also depends on progenitor orbit. A considerable iteration process is required in order to achieve a satisfying agreement with measurement results for all epochs as shown in Figure 8.

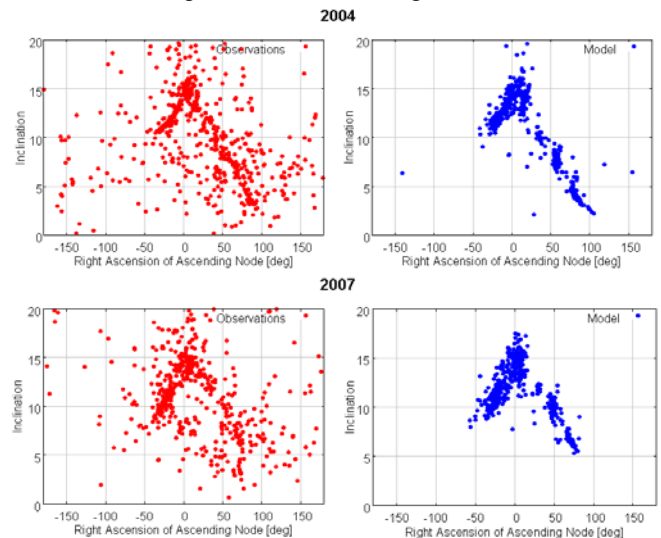


Figure 8: Measured (left) and modeled (right, incl. additional events) uncorrelated objects for the year 2004 (top) and 2007 (bottom)

Table 4 lists the real objects close to the progenitor orbits at the estimated time of the 8 additional events that have been defined. These objects are not necessarily hot candidates for the originators due to the mentioned ambiguities. Measurements from additional years are required in order to achieve a reliable correlation.

Table 4: Definition of the additional events used to match observations

Event epoch	Inclination	RAAN	Potential association
Mar. 1987	8.57°	57.48°	1975-118C
Jan. 1989	0.20°	349.10°	1987-100D, 1987-028D, 1987-073A, 1988-036A
Apr. 1991	9.60°	59.60°	
Jan. 1993	12.40°	50.10°	1975-100F
Jul. 1993	9.60°	59.60°	1981-069F, 1982-020F, 1984-028F
Aug. 1993	0.20°	349.10°	1991-046A, 1991-014A, 1991-079A
Sep. 1999	12.00°	25.710°	1975-177A
Oct. 1999	0.05°	74.320°	1994-082D, 1997-092C

From Figure 1 it is obvious that for the detections made during GTO surveys the model is showing substantial gaps. This is also evident in the number of detections which amounts to 596 in the model (compared to 928 in the measurement) in 2005. In the absence of any additional information the known fragmentation events in GTO have been enhanced in the model, leading to an increase of the number of fragments by a factor of 10.

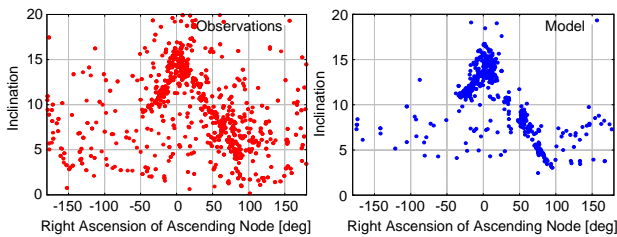


Figure 9: Measured (left) and modeled (right) uncorrelated objects for the year 2005 with enhanced number of modeled GTO fragments

The number of modeled detections now amounts to 682 in 2005. However, there is an obvious under-coverage of some orbit regions, in particular at low and very high inclinations. This could be due to either missing fragmentation events as for GEO or a significant source term is not yet considered.

### 3.3. High Area to Mass objects

A possible explanation for this unconsidered group of detections could be objects of very high area/mass ratios that seem to have been released from geostationary objects. These objects have been detected first by the ESA Space Debris Telescope [6] during standard GEO and GTO surveys. Follow-up campaigns and subsequent orbit determination of a subset of the detected objects revealed orbits of high eccentricities but geostationary

orbit periods. Observations of longer periods revealed that these orbits have very large ratios of area-to-mass. While typical spacecraft or fragments have area-to-mass ratios around  $0.01 \text{ m}^2/\text{kg}$ , the ratios of these objects range between 10 and  $60 \text{ m}^2/\text{kg}$ . This is also the explanation for their particular orbits which is a result of solar radiation pressure to which these objects are very sensitive. Figure 10 compares the evolution of inclination and RAAN of two objects on geostationary orbit with a very high and a very low area-to-mass ratio over a period of 52 years.

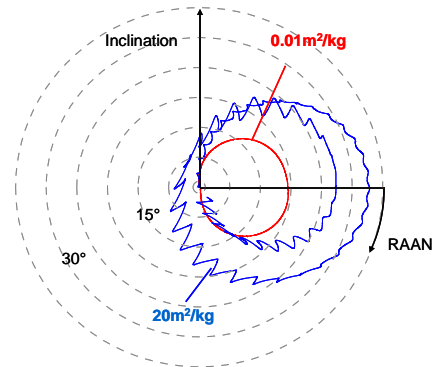


Figure 10: Orbital evolution of objects with A/m ratios of  $0.01 \text{ m}^2/\text{kg}$  and  $20 \text{ m}^2/\text{kg}$  over 52 years

While the dense object is following the behaviour expected for GEO objects with a 52 year period, the HAM object orbit is reaching a large inclination amplitude with a period of about half of that for the dense object. A shorter-term perturbation term with a period of 1 year is superimposed. The eccentricities reached during this process are generally large and follow the same shorter-term periodicity. The large eccentricity (that could even lead to decay) cause a larger influence of the luni-solar perturbation which is the reason for the larger amplitude in inclination.

A release model for these HAM objects has been developed in [5]. The model assumes that these objects are multi-layer insulation (MLI) foil that is used for thermal protection of spacecraft. MLI is a promising candidate since the area-mass-properties are close to that of the observed HAM pieces. The model considers two release mechanisms: delamination and break-up of spacecraft. Only three-axis stabilised spacecraft (and not upper-stages) are considered to be originators of MLI pieces. Existing spacecraft designs have been analysed in [5] for the amount and type of MLI used as well as for the number of layers. A review of literature on the MLI degradation process and reasonable engineering assumptions have lead to a release model for delaminated MLI as a function of the spacecraft age and to models for the distribution of piece sizes and a/M properties (release MLI pieces take different shapes from flat over rolled-up to near spherical) for both

release mechanisms. Figure 11 compares the combined modeling results including MLI pieces to the uncorrelated detections of 2005.

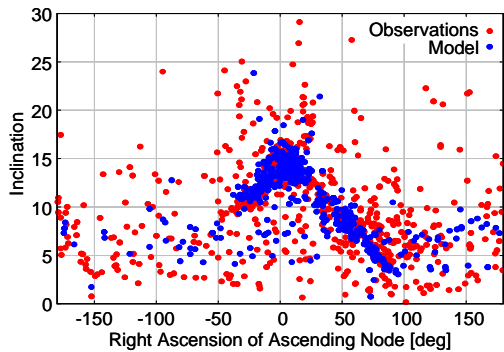


Figure 11: Measured (left) and modeled (right) uncorrelated objects for the year 2005 with including MLI fragments in the model

The number of modeled (856) and measured (928) detections is now reasonably close. Also the quality in the distribution had improved, which shows that released MLI pieces are a reasonable explanation for many of the observed objects. Additional adjustments are however still necessary in the next model release (MASTER-2009) to fully optimize the match.

### 3.4. Summary of changes to the model

The model calibration process triggered by the ESA Space Debris Telescope observations and described above will significantly improved the model predictions. Thanks to the measurements from the ESASDT, the model population could undergo a justifiable revision process leading to an enhancement by a factor 3 (compared to MASTER-99, which was published before the ESASDT measurement results have been available). Figure 12 compares the spatial density predictions of the model for the GEO region before and after the model adjustments. It is obvious that continuous space debris observations are essential for the quality of space debris models.

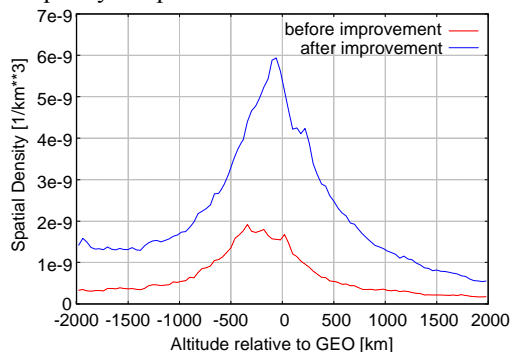


Figure 12: Change in the modeled spatial density before (MASTER-99) and after improvement

## 4. Conclusions

The GEO and GTO surveys of the ESA Space Debris Telescope revealed a considerable population of objects that cannot only be explained by so-far unknown fragmentation events. ESA's MASTER model had to be adjusted by the introduction of additional fragmentation events on GEO and by an enhancement of the number of objects released during GTO fragmentations. It became obvious that a remaining group of objects with unusual high A/m on highly eccentric orbits and geostationary period cannot be explained by fragmentation events. Pieces of MLI released by (in particular) delamination or during fragmentations are a good explanation for these objects. Accordingly, the model for MLI release should be extended and validated for the next model update (MASTER-2009). An analysis revealed that objects on Molniya orbits have the potential to interfere with the GEO protected region. These highly inclined orbits could be interesting targets for future observation campaigns.

## 5. References

- [1] Krag H., Bendisch J., Rosebrock J., Schildknecht T., Sdunnus H. "Sensor Simulation for Debris Detection" Final report ESA Contract 14708/00/D/HK, ILR/TUBS Braunschweig, 2002
- [2] Oswald M., Stabroth S., Wiedemann C., Wegener P., Martin C., Klinkrad H. "Upgrade of the MASTER Model", Final Report ESA contract 18014/03/D/HK(SC), 2006
- [3] Oswald M. "New Contributions to space Debris Environment Modeling" Dissertation, ZLR-Forschungsbericht 2008-03, Shaker Verlag, ISBN 978-3-8322-7172-5, Braunschweig, Germany, 2008
- [4] Johnson N. L., Stansbery E., Whitlock D. O., Abercromby K. J., Shoots D. "History of on-orbit satellite fragmentations", 14th Edition NASA Orbital Debris Program Office, NASA/TM-2008-214779, Houston, Texas 77058, USA, June 2008,
- [5] Flegel S. K. "Modelling the High-Area-to-Mass Ratio Debris Population in GEO", Studienarbeit R-0603-S, June 2006, Braunschweig, Germany
- [6] Schildkecht T., Musci R., Serra Ricart M., de Leon Cruz J., Domniguez Palmero L., Feltrami P., Bunte K.D. "Geostationary Transfer Orbit Survey" Final Report to ESA/ESOC Contract 12568/97/D/IM, December 2006, Berne, Switzerland